MECHANICS AND MECHANICAL ENGINEERING
International Journal
Vol. 5 No. 2 2001

EXPERIMENTAL AND ANALYTICAL INVESTIGATION OF ACTIVELY DAMPED BEAM VIBRATIONS

Marek Pietrzakowski
Warsaw University of Technology
Institute of Machine Design Fundamentals
Narbutta 84, 02-524 Warszawa, Poland
Tel. 48 (22) 660 86 23, E-mail: mpietrz @ ipbm.simr.pw.edu.pl

Abstract

The problem of active damping of cantilever beam transverse vibrations is considered, by using a collocated piezoceramic sensor and actuator. Experimental results of free vibrations confirmed the effectiveness of the control circuit with the analog derivative controller for suppression of a low-frequency beam motion. Theoretical analysis is based on the simplified pure bending model of interaction between the piezoactuator and the beam with a constant equivalent stiffness. The viscoelastic material parameters of the tested beam are estimated considering the fundamental frequency and logarithmic decrement of transient vibrations. The results of simulation, even for the applied simplified model of the system, are in a good agreement with the experiment.

1. Introduction

Piezoelectric materials such as lead zirconate titanate (PZT) ceramics and vinylidene fluoride (PVDF) polymers become popular in the use for a flexible structure controlling. Applications of distributed piezoelectric sensors and actuators for active damping of beams and thin plates are investigated theoretically and verified experimentally by many researches ([1], [2], [4] among others). The analysis is commonly based on a pure bending interaction of a perfectly bonded mass less actuator (cf. [1], [2], [3], [6], [7]). The static approach is a simplification of the coupling model but occurs quite reasonable for piezoelectric patches or layers which mass can be ignored in the system motion description (cf.[5]).

In this paper, the control system with piezoceramic sensors and actuators designed for active damping of a cantilever beam is experimentally tested and analyzed theoretically. Experiments show that the beam vibrations are reduced significantly by using the analog control circuit with velocity feedback. Numerical simulations performed using the static coupling model confirm experimental results of the free vibration control.

2. Experimental arrangement

To test the active damping of vibration using a piezoelectric control system, experiments were performed on a cantilever beam. The geometry of the tested beam is shown in Fig. 1.

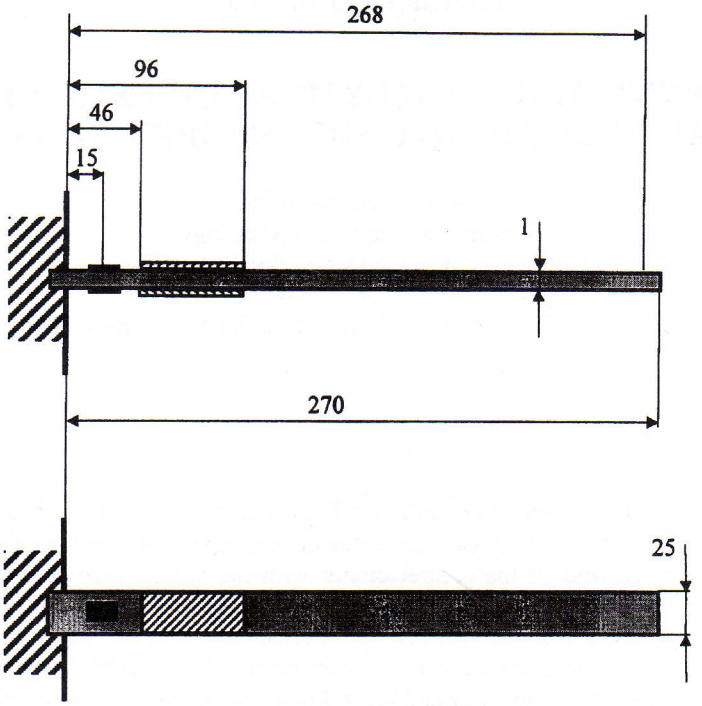

Fig.1. Schematic of the tested beam

The beam is constructed of stainless steel strip of length $l = 270$ mm, width $b = 25$ mm and thickness $t_b = 1$ mm, clamped at one end and free at the other. The sensor and actuator formed by a pair of piezoceramic patches are bonded on opposite sides 46 mm from the root of the beam. The pair of "QickPack" piezoceramic transducers is used, QP10N type (50.8 × 25.4 × 0.381 mm) as the actuator and QP15N type (50.8 × 25.4 × 0.254 mm) as the sensor [8]. They are attached to the beam surface using a two-part epoxy resin recommended for "QickPack" products.

The experimental investigation concerned suppression of the transient vibrations referred to the first-mode. The fundamental frequency of the beam with the piezoceramic patches was experimentally obtained to be $\omega_1 = 73.8$ 1/s (11.75 Hz).

The control loop is composed using analog techniques. The signal from the piezosensor is fed to a pre-amplifier and then is transformed by the derivative (D) controller due to the velocity feedback control strategy. Differentiation of the sensor signal introduces time delay in the control system, which can be significant for higher natural frequencies. Therefore, filtering is necessary to remove the high-frequency components of the control signal to avoid instability of the beam vibrations. The RC filter is installed between the pre-amplifier and the controller and is designed to eliminate any electrical signal with frequencies above 200 1/s (≈32 Hz). The signal from the controller is finally amplified via the power amplifier and is then fed to the actuator to generate control response to suppress the vibrations.

For the detection of the beam motion, a strain gauge system mounted near the clamped end is applied. The signal from the gauges working in a half bridge is sent to the measure amplifier (Spider 8 from HBM) with analogue to digital (AD) converter installed and then recorded on a hard disk on PC. The "Catman" data acquisition system is used for analyzing data and visualizing results.

The experimental setup for active control of the cantilever beam is presented in Fig. 2.

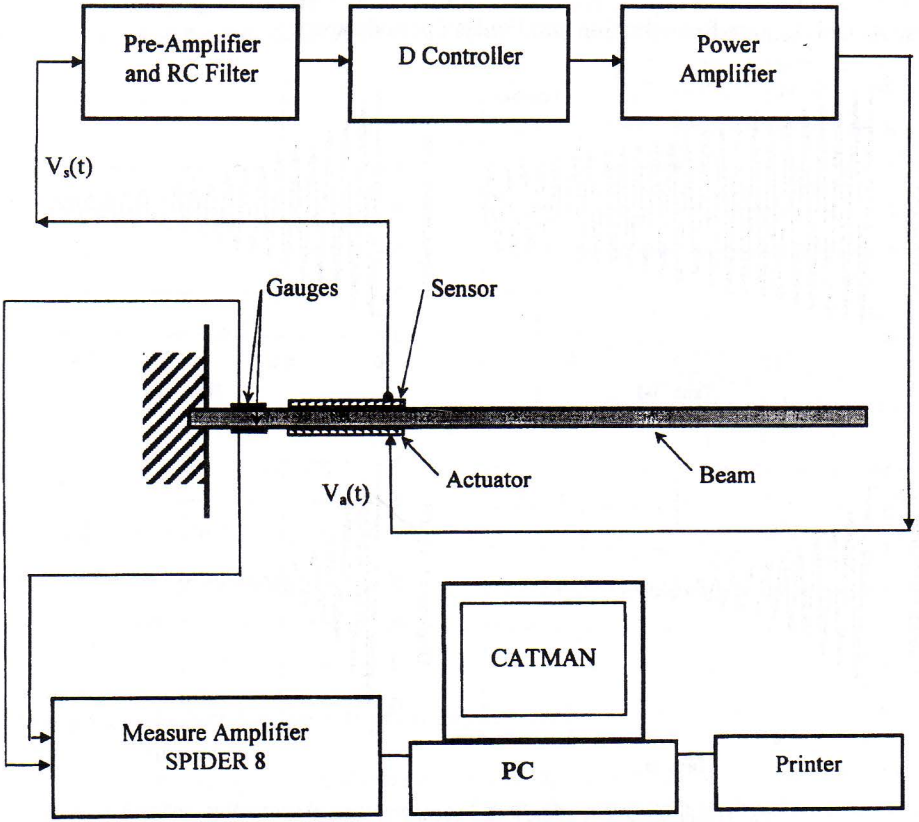

Fig. 2. Experimental setup

Experiments were performed on the free vibrations of the beam; first without and then with the active control system. The motion of the near-tip beam point at 2 mm from the free end is detected.

For an initiation of free vibrations the tip of the beam is deflected by about 3 mm and then released. The transient vibrations of the beam point represented uncontrolled system and the actively damped beam with the various control gain κ are shown in Fig. 3. The control gain κ is defined as a ratio of the magnitude of the output voltage V_a applied to the actuator and the input voltage V_s generated by the sensor, $\kappa = V_a / V_s$. It can be clearly noticed that the damping ratio increases significantly with an increase of the control gain parameter. But the control system effectiveness is limited because of the high vibration modes, which are generated for sufficiently great values of the gain.

The passive damping observed for uncontrolled beam response (see Fig. 3) is combined effects due to material damping, air damping and damping created by the measuring equipment. The level of the high frequency components is low for the uncontrolled as well as controlled vibrations mainly due to the low-pass filter installed in the control circuit. Therefore, estimation of the damping coefficient, both for passive and active cases, can be based on the classical logarithmic decrement concept. The logarithmic decrement δ is expressed by the well-known relation

$$\delta = \frac{1}{i} \ln \frac{A_n}{A_{n+i}} \tag{1}$$

where A_n and A_{n+1} are free vibration amplitudes i periods apart.

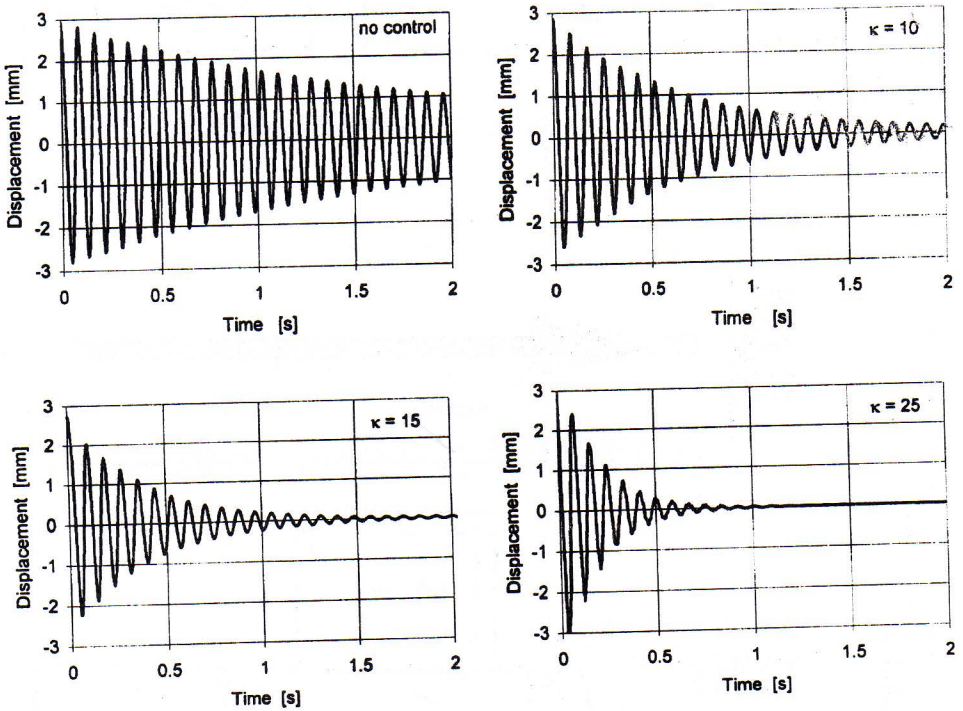

Fig. 3. Free vibrations of the tested beam without and with active damping. Effects of passive damping and variation in the control gain

Results of the logarithmic decrement calculations for passively damped transient vibrations are presented in Fig. 4.

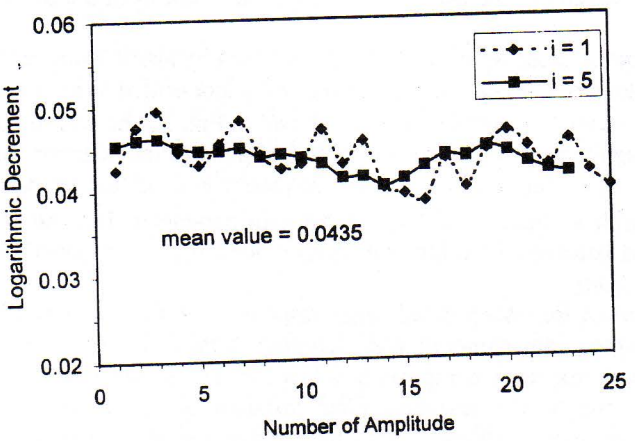

Fig. 4. Evaluation of passive damping

The doted line is obtained for amplitudes recorded after the period (i = 1). Differences between the values of the logarithmic decrement are caused by the measurement errors and also by the influence of the second and higher modes on the beam response. The solid line refers to the averaged logarithmic decrement computed for the sequence of peaks 5 periods apart (i = 5). Taking into account the locally averaged values, the mean loga-

rithmic decrement, which quite well approximates energy dissipation of the tested beam, is determined as $\delta = 0.0435$.

The active damping effectiveness depending on the control gain is shown in Fig. 5. In this case the mean logarithmic decrement is calculated for the sequential amplitudes 1 period apart. The number of recorded peaks varied from 5 to 15 for the high and low control gain, respectively. The plot shows that the damping intensity increases slightly for the low and high control gain and the logarithmic decrement rate is maximal for the middle values of the applicable gain range ($\kappa = 15 - 20$).

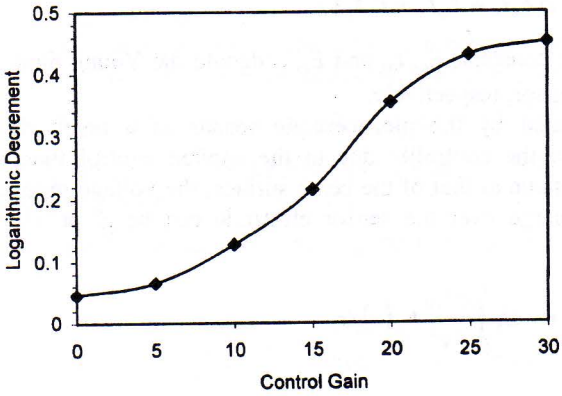

Fig. 5. Logarithmic decrement vs. the control gain

Experimental results both for the excited and the free vibrations show that the active damping effect is evident. As expected, the intensity of reduction of the free vibration amplitude increases significantly for a greater control gain parameter. A disadvantage of the used analog control system is an excitation of the high vibration components observed for the extremely great gain values.

3. Theoretical relations for the actively damped beam

The dynamic analysis of the considered system can be simplified by imposing the static pure bending model of coupling between the beam and the perfectly bonded piezoelement. Due to this model the actuator action caused by the applied voltage is reduced to bending moments at both ends of the piezoceramic patch. The transverse motion of the controlled viscoelastic beam with a uniform bending stiffness and mass density, which is excited by the point force $F(t)$ can be described as follows

$$E_b J_b \left(\frac{\partial^4 w}{\partial x^4} + \mu \frac{\partial^5 w}{\partial x^4 \partial t} \right) + \rho_b b t_b \frac{\partial^2 w}{\partial t^2} = F(t)\delta(x - x_f) - \frac{\partial^2 M_a(x,t)}{\partial x^2} \tag{2}$$

where E_b, J_b indicate the beam Young modulus and the cross-sectional moment of inertia, respectively, b, t_b,ρ_b are the beam width, thickness and mass density, respectively, μ is the viscous internal damping parameter of Voigt-Kelvin model, x_f is the co-ordinate of the point force, $\delta(x)$ denotes the Dirac function.

The bending moment $M_a(x,t)$ is distributed along the actuator and can be calculated taking into account the constitutive equation of the piezoelectric material and the moment equilibrium of the resultant forces acting in the cross-section of the beam (cf. [1], [6] among others)

$$M_a(x,t) = C_a b_p(x) V_a(t) \tag{3}$$

where $V_a(t)$ is the voltage applied to the actuator, $b_p(x)$ is the piezoelectric patch width distribution described using the Heaviside function, $b_p(x)=b[H(x-x_1)-H(x-x_2)]$, C_a is the actuator constant given by the relation

$$C_a = \frac{d_{31}^a E_a E_b \left(t_b^2 + t_a t_b\right)}{2\left(E_b t_b + E_a t_a + E_s t_s\right)} \tag{4}$$

where d_{31}^a is the actuator piezoelectric constant, E_a, t_a, and E_s, t_s denote the Young modulus and thickness of the actuator and the sensor, respectively.

The input voltage $V_a(t)$ is generated by the piezoceramic sensor as a result of its deformation and then transformed via the controller due to the applied control function. Assuming the sensor strains to be the same as that of the beam surface, the voltage produced by the sensor after integrating the charge over the sensor electrode can be given by the integral

$$V_s(t) = -C_s \int_0^l \frac{\partial^2 w}{\partial x^2} b_p(x) dx \tag{5}$$

where C_s is the sensor constant

$$C_s = d_{31}^s E_s \frac{\left(t_b + t_s\right)}{2C} \tag{6}$$

where d_{31}^s is the sensor piezoelectric constant, C is the total sensor capacitance, $C = A_s e_{33} / t_s$, with A_s – sensor electrode area, e_{33} – permittivity of the sensor material.

Assuming velocity feedback and after substituting Eq. (4) the control bending moment, Eq. (3), can be rewritten as follows

$$M_a(x,t) = k_d C_a C_s b_p(x) \int_0^l \frac{\partial^3 w}{\partial x^2 \partial t} b_p(x) dx \tag{7}$$

where k_d is the velocity gain factor of the control loop.

The response of the actively damped beam subjected to a harmonic excitation can be expressed in terms of transfer function. The block diagram with the velocity feedback is shown in Fig. 6.

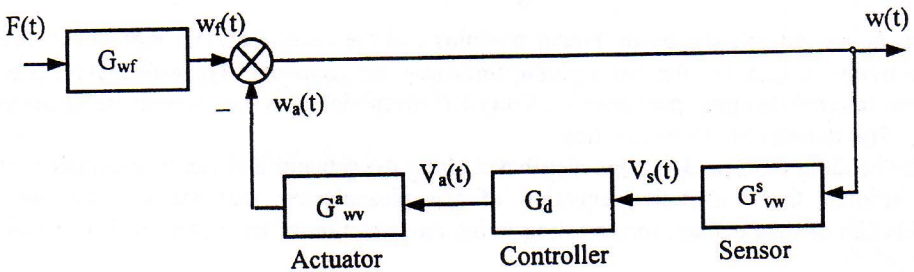

Fig. 6. Block diagram of the system

where $V_a(t)$ is the voltage applied to the actuator, $b_p(x)$ is the piezoelectric patch width distribution described using the Heaviside function, $b_p(x)=b[H(x-x_1)-H(x-x_2)]$, C_a is the actuator constant given by the relation

$$C_a = \frac{d_{31}^a E_a E_b \left(t_b^2 + t_a t_b\right)}{2\left(E_b t_b + E_a t_a + E_s t_s\right)} \tag{4}$$

where d_{31}^a is the actuator piezoelectric constant, E_a, t_a, and E_s, t_s denote the Young modulus and thickness of the actuator and the sensor, respectively.

The input voltage $V_a(t)$ is generated by the piezoceramic sensor as a result of its deformation and then transformed via the controller due to the applied control function. Assuming the sensor strains to be the same as that of the beam surface, the voltage produced by the sensor after integrating the charge over the sensor electrode can be given by the integral

$$V_s(t) = -C_s \int_0^l \frac{\partial^2 w}{\partial x^2} b_p(x) dx \tag{5}$$

where C_s is the sensor constant

$$C_s = d_{31}^s E_s \frac{\left(t_b + t_s\right)}{2C} \tag{6}$$

where d_{31}^s is the sensor piezoelectric constant, C is the total sensor capacitance, $C = A_s e_{33} / t_s$, with A_s – sensor electrode area, e_{33} – permittivity of the sensor material.

Assuming velocity feedback and after substituting Eq. (4) the control bending moment, Eq. (3), can be rewritten as follows

$$M_a(x,t) = k_d C_a C_s b_p(x) \int_0^l \frac{\partial^3 w}{\partial x^2 \partial t} b_p(x) dx \tag{7}$$

where k_d is the velocity gain factor of the control loop.

The response of the actively damped beam subjected to a harmonic excitation can be expressed in terms of transfer function. The block diagram with the velocity feedback is shown in Fig. 6.

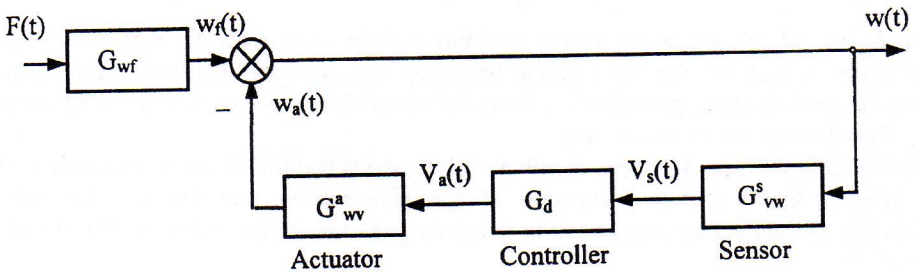

Fig. 6. Block diagram of the system

The steady-state solution to Eq. (2) can be written using the modal superposition

$$w(x,t)=\sum_{n=1}^{\infty}C_nW_n(x)\exp(i\omega t) \tag{8}$$

where C_n are the amplitude coefficients, ω is the frequency of excitation, $W_n(x)$ denote the modal shape functions.

The modal functions are determined by the boundary conditions and for a cantilever beam of length l heaving one end fixed and other free are expressed in the well-known form

$$W_n(x)=(\sin k_nl+\sinh k_nl)(\cosh k_nx-\cos k_nx)-(\cos k_nl+\cosh k_nl)(\sinh k_nx-\sin k_nx) \tag{9}$$

where k_n are the roots of the frequency equation $\cos k_nl\cosh k_nl=-1$ with the values of $k_nl=$ 1.875, 4.694, 7.855,..., $0.5(2n-1)\pi$.

The transfer function G_{wf} relating the beam deflection to the loading force is given by the formula

$$G_{wf}(x,\omega)=\frac{w(x,\omega)}{F(\omega)}=\frac{1}{\rho_bbt_b}\sum_{n=1}^{\infty}\frac{W_n(x_f)W_n(x)}{\gamma_n^2(\omega_n^2-\omega^2+i\mu\omega_n^2\omega)} \tag{10}$$

where ω_n is the nth natural frequency

$$\omega_n=k_n^2\sqrt{\frac{E_bJ_b}{\rho_bbt_b}} \tag{11}$$

and $\gamma_n^2=\int_0^lW_n^2(x)dx$.

The transfer function of the output beam deflection to the input actuator voltage can be obtained in the form

$$G_{wv}^a(x,\omega)=\frac{w(x,\omega)}{V_a(\omega)}=\frac{C_a}{\rho_bbt_b}\sum_{n=1}^{\infty}\frac{T_nW_n(x)}{\gamma_n^2(\omega_n^2-\omega^2+i\mu\omega_n^2\omega)} \tag{12}$$

where T_n is the actuator shape factor

$$T_n=\int_0^l\frac{d^2b_p(x)}{dx^2}W_n(x)dx=b\left(\frac{dW_n(x)}{dx}\Big|_{x_2}-\frac{dW_n(x)}{dx}\Big|_{x_1}\right) \tag{13}$$

The output voltage of the sensor caused by the beam deflection is given by the relation

$$G_{vw}^s(x,\omega)=\frac{G_{vf}^s(\omega)}{G_{wf}(x,\omega)} \tag{14}$$

where G_{vf}^s describes the response of the sensor voltage to the input external force and has the form

$$G_{vf}^s(\omega)=\frac{V_s(\omega)}{F(\omega)}=\frac{C_s}{\rho_bbt_b}\sum_{n=1}^{\infty}\frac{S_nW_n(x_f)}{\gamma_n^2(\omega_n^2-\omega^2+i\mu\omega_n^2\omega)} \tag{15}$$

Considering velocity feedback, the controller transforms the input voltage signal according to the relation

$$G_d(\omega) = ik_d\omega \tag{16}$$

where k_d is the derivative gain factor.
The closed-loop transfer function of the controlled beam is given by the well-known equation

$$G_c = \frac{G_{wf}}{1+G_o} \tag{17}$$

where G_o is the open-loop transfer function defined as the following product

$$G_o = G_{vw}^s G_d G_{wv}^a \tag{18}$$

Free vibrations of the beam can be analyzed using the impulse transfer function. The time-response of the system to the impact $F(t) = \delta(t)$ is defined as the inverse Fourier transform of the transfer function $G_c(x, \omega)$

$$h_c(x,t) = \frac{1}{2\pi}\int_{-\infty}^{\infty} G_c(x,\omega)\exp(i\omega t)d\omega \tag{19}$$

4. Results of simulation

The numerical simulation was performed for the model of the system which geometry is described in the Chapter 2. It is assumed that the Young modulus of the stainless steel beam is $E_b = 2.05\times10^{11}$ N/m^2. The material viscous damping parameter (Voigt-Kelvin model) is calculated for free vibrations of the tested beam due to the relation $\mu = \delta/(\pi\omega_1)$. Substituting the fundamental frequency $\omega_1 = 73.8$ 1/s and the mean logarithmic decrement $\delta = 0.0435$, the damping parameter is estimated to be $\mu = 1.88\times10^{-4}$ s.

Applying the simple static coupling model with the constant stiffness and mass density along the beam (Chapter 3), the Young modulus is derived to be $E_b = 2.19\times10^{11}$ N/m^2 in order to match the theoretical first natural frequency of the beam with the measured one. This is justified because of the local stiffening effect of the piezoceramic patches.

Electro-mechanical parameters of the piezoceramic transducers are determined basing on the technical data given in [8]. The equivalent Young modulus of the actuator and sensor patches are calculated applying the mixture rule for the piezoceramic PZT material with $E_p = 6.3\times10^{10}$ N/m^2 and the resin covering with $E_m = 2.8\times10^9$ N/m^2. The piezoelectric coefficient d_{31} refers to the linear estimation of the strain-voltage characteristic of the piezoceramic devices for voltage amplitudes less then 60 V. The electro-mechanical parameters used in calculation are listed in Table 1.

Table 1. Material parameters of transducers

Material Parameter	Actuator QP10N	Sensor QP15N
ρ (kg/m^3)	5780	6900
E (N/m^2)	3.3×10^{10}	2.5×10^9
d_{31} (m/V) or (C/N)	2.3×10^{-10}	2.5×10^{-10}
C (μF)	0.06	0.10

To obtain free vibrations the beam end is subjected to an impulse excitation. The beam response is calculated at the measure point (x = 268 mm) according to Eq. (19) derived for the simplified model. For comparison of the simulation and experimental results the impulse value is determined by matching the beginning response amplitudes with the initial displacement of the tested

beam. The results of simulation obtained for the uncontrolled system and for several values of the gain factor $k_d = 0.135$ s ($\kappa = 10$), $k_d = 0.203$ s ($\kappa = 15$), $k_d = 0.338$ s ($\kappa = 25$), are presented in Fig. 7. As mentioned above, the passive damping refers to Voigt-Kelvin model with the retardation time $\mu = 1.88 \times 10^{-4}$ s which quite well describes the energy dissipation of the tested beam (compare Fig. 7 with Fig. 3). For the actively damped beam the effect of the gain factor increasing is evident. Comparing the results of the simulation with the free vibration plots obtained experimentally, it can be noticed that the active damping effect is generally similar but it is stronger for the theoretical evaluation. The reason for this behavior is the applied simple model of the system with the additional stiffness of the activated segment neglected and the perfect bonding assumed.

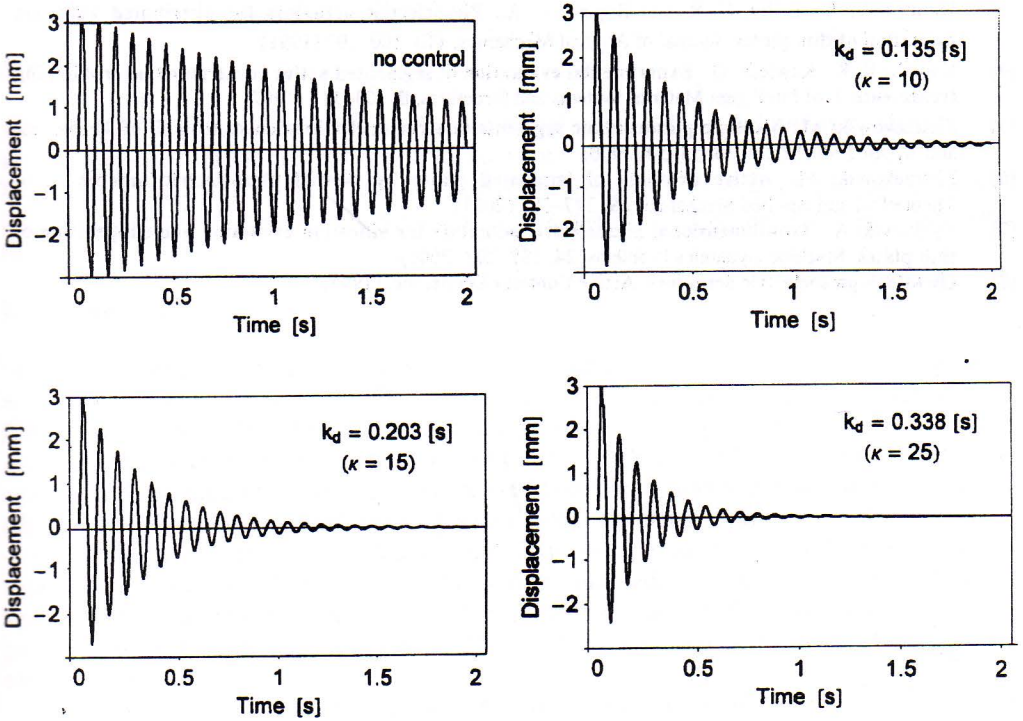

Fig. 7. Impulse response of the beam without and with active damping. Effects of passive damping and variation in the control gain.

5. Final remarks

The active damping technique using piezoceramic sensors and actuators was demonstrated by the experiment and described theoretically. The investigation was focused on a suppression of low frequency vibrations of the cantilever beam. The experimental results of free vibrations confirmed that even a simple analog feedback with the derivative controller is effective for the active damping of the beam transverse motion. Increasing the gain of the control circuit can significantly increase the rate of the vibration reduction. In practice, the gain values are limited because of the tendency of the control system to amplify unwanted

high vibration components. The simulation results showed a quite good agreement with the experiment even for the simplified model of the controlled beam. The model quality can be improved by taking into account the local stiffening of the activated beam and by considering the dynamic model of interaction between the actuator and the beam.

References

[1] Bailey, T., Hubbard, J. E.: **Distributed piezoelectric-polymer. Active vibration control of a cantilever beam**. Journal of Guidance, Control and Dynamics, **8**, 605–611 (1985)

[2] Clarc, R. L., Fuller, Ch. R., Wicks, A.: **Characterization of multiple piezoelectric actuators for structural excitation**. *J.Acoust. Soc.Am.*, **90**, 346–357 (1991)

[3] Dimitriadis, E., Fuller, C. R. and Rogers, C. A.: **Piezoelectric actuators for distributed vibration excitation of thin plates**. Journal of Applied Mechanics, **113**, 100–107 (1991)

[4] Kapadia R. K., Kawiecki G.: **Experimental evaluation of segmented active constrained layer damping treatments**. J. of Intelligent Material Systems and Structures, **8**, 103–111 (1997)

[5] Pietrzakowski M.: **Multiple piezoceramic segments in structural vibration control**. J. of Theoretical and Applied Mechanics, **38**, 35–50 (2000)

[6] Pietrzakowski M.: **Active damping of laminated plates by skewed piezoelectric patches**. J. of Theoretical and Applied Mechanics, **39**, 377–393 (2001)

[7] Tylikowski A.: **Two-dimensional piezoelectric actuators for vibration excitation and suppression of thin plates**. Machine Dynamics Problems, **24**, 199–207 (2000)

[8] **QickPack piezoelectric actuators**. Active Control eXperts, Inc. (1997)